

## Weakly Dispersive Band near the Fermi Level of GaMnAs Due to Mn Interstitials

A. Ernst,<sup>1,\*</sup> L. M. Sandratskii,<sup>1</sup> M. Bouhassoune,<sup>1</sup> J. Henk,<sup>1</sup> and M. Lüders<sup>2</sup>

<sup>1</sup>Max-Planck-Institut für Mikrostrukturphysik, Weinberg 2, D-06120 Halle (Saale), Germany

<sup>2</sup>Daresbury Laboratory, Daresbury, Warrington, WA4 4AD, United Kingdom

(Received 22 August 2005; published 29 November 2005)

The nature of the weakly dispersive electronic band near the Fermi level observed in photoemission experiments on the diluted magnetic semiconductor GaMnAs is investigated theoretically. The combination of experimental features appears puzzling. We show that the formation of the band is closely related to the presence of the Mn interstitial impurities. The states forming the band have predominantly minority-spin Mn-3*d* character. The low experimental Mn-3*d* intensity is explained by the low content of the interstitial Mn impurities. The features of the band are robust with respect to the calculational technique [local density approximation (LDA), LDA + *U*].

DOI: 10.1103/PhysRevLett.95.237207

PACS numbers: 75.50.Pp, 61.43.Bn, 61.66.Dk, 71.55.Eq

Because of the combination of magnetic and semiconducting properties, diluted magnetic semiconductors (DMS) possess a high potential for spin-electronic applications [1]. To date, the largest effort of research was devoted to GaMnAs, which might be considered as the paradigmatic DMS. Intensive studies of GaMnAs were stimulated by experimental detection [2] of the ferromagnetism with Curie temperature  $T_c$  as high as 110 K for a Mn concentration of  $x = 5.3\%$ . With further advances in sample preparation,  $T_c$  could be increased up to 159 K [3].

Despite these successes, the nature of the ferromagnetism in GaMnAs is still a matter of controversy. In general, it is agreed upon that the presence of the charge carriers, i.e., of partially filled electronic bands, is crucial for the formation of the ferromagnetism. However, the various models proposed differ in how the effective exchange interaction between the Mn impurities is mediated by these states. On the one hand, it is argued that the ferromagnetism of GaMnAs can be described in terms of the Zener model [4], assuming a hostlike character of the hole states. These states become spin-polarized by the exchange field of the localized Mn-3*d* moments and, therefore, are able to mediate the effective exchange interaction between Mn atoms. Other models suggest that the leading mechanism is double exchange [5]. In this scenario, a strong Mn-3*d* contribution to the charge-carrier states is required. Therefore, the energy position of the Mn-3*d* states is a key issue for understanding the magnetism of this system.

One of the prominent tools to study electronic structures is angle-resolved photoelectron spectroscopy, which provides detailed information on the occupied electronic states [6]. The valence band structure of Ga<sub>1-x</sub>Mn<sub>x</sub>As with Mn concentrations  $x = 0.035$  and  $0.069$  was studied by Okabayashi *et al.* [7] One remarkable result of their experiments is the presence of a weakly dispersive band along the  $\Gamma$ - $\Delta$ - $X$  high-symmetry line of the Brillouin zone with 0.5 eV binding energy, which is apparently induced by Mn since it is absent in the undoped semiconductor. Contrary to expectations for a weakly dispersive band, the experimental photoemission intensity of the Mn-3*d*

states in the corresponding energy region is low. The authors speculate that the associated electronic states consist mainly of As-4*p* orbitals with a small admixture of Mn-3*d* states. Considering the strong dispersion of the GaAs-host bands, the formation of a weakly dispersive band constituted of electronic states of the semiconductor matrix seems puzzling.

The observation of the weakly dispersive energy band near Fermi level not only offers a challenging physical problem, it is also important with respect to spintronic applications since electronic states close to the Fermi level modify strongly the electronic transport. Thus, it appears necessary to understand the origin and properties of the weakly dispersive band. In this Letter, we report the results of an extensive first-principles investigation of the electronic structure of GaMnAs, focusing on the formation and properties of the weakly dispersive band. The *ab initio* calculations reported so far did not provide information on this band.

Electronic structure was computed using the Korringa-Kohn-Rostoker method [8]. Most of the calculations are performed within the local density approximation (LDA) to density-functional theory. In some calculations, the LDA + *U* technique is used. The calculations were performed for Mn concentration  $x = 0.035$ . The disorder in the positions of the Mn impurities was treated within the coherent potential approximation (CPA). By this means, the site- (*s*) and spin- ( $\tau$ ) resolved Bloch spectral density  $N_s^\tau(E, \mathbf{k})$  becomes broadened, as compared to the ordered case [8]. To make the link to the familiar band structure  $E(\mathbf{k})$ , the positions of distinct maxima in  $N_s^\tau(E, \mathbf{k})$  are presented in the following as a function of wave vector  $\mathbf{k}$ . Here  $E$  is the energy of the electronic state.

The major effect of doping of GaAs by Mn is expected from Mn impurities substituting Ga atoms. Most of the theoretical investigations were performed for this structural model. Therefore, in our initial calculations ferromagnetic (Ga<sub>1-x</sub>Mn<sub>x</sub>)As with Mn impurities occupying only Ga positions was assumed, too (for short, *S* for *substitutional* alloy). The resulting band structure for the

$\Gamma$ - $\Delta$ - $X$  line (dots in Fig. 1) follows closely that of the GaAs host (solid lines). The weakly dispersive structure at about  $-3$  eV (relative to  $E_F = 0$  eV) in the majority-spin channel is related to  $3d^1$  states of Mn. Upon approaching the semiconductor bands, its spectral density gets broader and can hardly be identified. The energy position of the Mn- $3d^1$  band at about  $-3.0$  eV is close to the photoemission result reported by Åsklund *et al.* [9] but somewhat higher than the experimental position of the corresponding states measured by Okabayashi *et al.* [10] ( $-4.5$  eV) and Rader *et al.* [11] ( $-4.3$  eV). Okabayashi *et al.* and Rader *et al.* explained the difference between the measured and the theoretical values by an insufficient account for the on-site correlations within the LDA approach (see further discussion at the end of the Letter).

The minority counterpart of these states is obtained above the Fermi energy at  $+0.3$  eV [Fig. 1(b)]. Most important for us: The nondispersive band observed in experiment at  $-0.5$  eV (crosses at  $-0.5$  eV in Fig. 1) is not reproduced by these calculations.

One reason for this failure might be the influence of the magnetic fluctuations on the electron structure. Indeed, the experiments were performed at room temperature that is significantly larger than the Curie temperature. On the other hand, the calculations were carried out for the ferromagnetic ground state. The paramagnetic state of the system of well-defined atomic moments can be described on the basis of the disordered local moment (DLM) approach [12]. Within this approach, the random orientations of the Mn magnetic moments above  $T_c$  are modeled with the use of the CPA as random alloy  $(\text{Ga}_{1-x}\text{Mn}_{x/2}^+ \text{Mn}_{x/2}^-) \text{As}$ , where  $\pm m$  give the projection of the atomic Mn moment on the spin-quantization axis. Since the net magnetization van-

ishes, spin- $\uparrow$  and  $-\downarrow$  electron structures coincide. On the other hand, the local Mn moment does not change substantially under transition from the ferromagnetic state to the paramagnetic state. As a result, the total density of states is very similar in both paramagnetic and ferromagnetic cases. The electron energy bands, present in the ferromagnetic state in one of the spin channels, in the paramagnetic phase are obtained in both spin channels with half value of the spectral weight. Therefore, the magnetic disorder does not lead to the appearance of the bands at new energy positions. In summary, the substitutional structure  $S$  neither in the ferromagnetic nor in the paramagnetic phase can explain the experimental results.

Recently, experimental evidence was reported that, depending on sample preparation, Mn can occupy interstitial positions of the GaAs host [13]. The question arises whether the nondispersive band is related to the presence of interstitial Mn. In the zinc-blende structure, there are two interstitial positions, which could be occupied by Mn: one surrounded by a cation tetrahedron (denoted as  $C$ , green in Fig. 1), the other position by an anion tetrahedron (structure  $\mathcal{A}$ , yellow in Fig. 1).

A number of calculations for systems containing both substitutional and interstitial Mn were performed (for short,  $S + I$ , where  $I = C$  or  $\mathcal{A}$ ). The sum of concentrations of the substitutional Mn atoms,  $x_S$ , and interstitial Mn atoms,  $x_I$ , was fixed to 0.035. Both parallel (denoted as FM) and antiparallel (denoted as AFM) orientations of the magnetic moments of the substitutional and interstitial impurities were considered (cf. Table I).

In Figs. 1(c) and 1(d), the band structure of  $(\text{Ga}_{0.965}\text{Mn}_{0.03}^S)\text{Mn}_{0.005}^C\text{As}$  in ferromagnetic configuration is depicted for minority electrons. As for structure  $S$

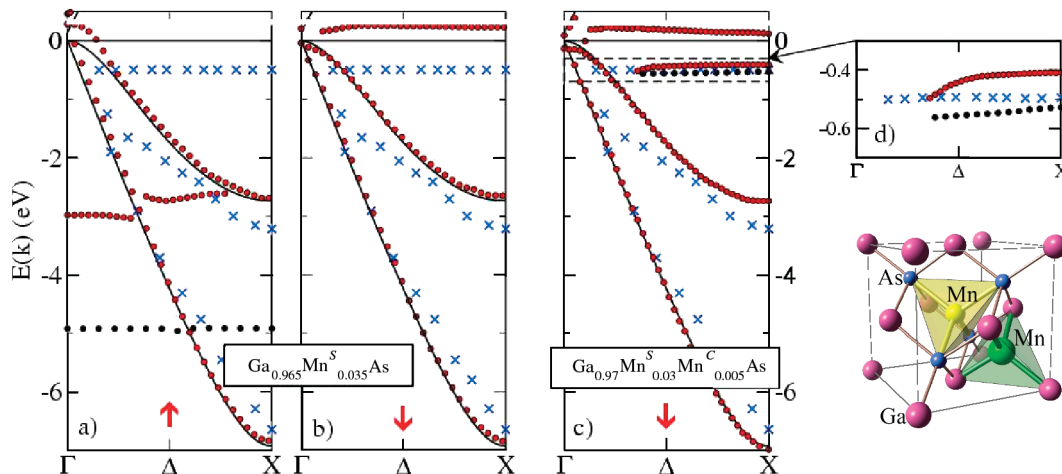


FIG. 1 (color). Panels (a) and (b): Spin-resolved electronic structure of  $\text{Ga}_{0.965}\text{Mn}_{0.035}\text{As}$  with Mn substituting Ga along  $\Gamma$ - $\Delta$ - $X$  [(a) majority spin; (b) minority spin]. The dots mark maxima in the Bloch spectral density. The crosses present the experimental data from Ref. [7]. Panel (c): The minority-spin band structure for  $\text{Ga}_{0.965}\text{Mn}_{0.03}^S\text{Mn}_{0.005}^C\text{As}$ . The inset (d) presents in a larger scale the weakly dispersive band near the Fermi level. In all figures, the red circles present the results of the LDA calculations. The black circles show bands obtained with the LDA +  $U$  method. The left bottom part of the picture: Cubic unit cell of the GaAs zinc-blende structure. Two interstitial Mn sites are arranged along a cube diagonal: Interstitial Mn atoms are placed within a Ga tetrahedron [cation ( $C$ ), green] or within an As tetrahedron [anion ( $\mathcal{A}$ ), yellow].

TABLE I. Atomic magnetic moments (in Bohr magneton  $\mu_B$ ) of Mn in GaMnAs for Mn substituting Ga (magnetic moment  $m_S$  and concentration  $x_S$ ) and interstitial Mn (magnetic moment  $m_I$  and concentration  $x_I$ ;  $I = \mathcal{A}, \mathcal{C}$ ; cf. Fig. 1). In the cases  $S + I$ , data for both FM and AFM configurations of the Mn moments  $m_S$  and  $m_I$  are presented. The results for  $S$  are in agreement with previous calculations [14–16].

Structure	Configuration	$m_S$	$x_S$	$m_I$	$x_I$
$S$	FM	3.69	0.035	...	...
$S + \mathcal{A}$	FM	3.78	0.030	3.03	0.005
$S + \mathcal{A}$	AFM	3.74	0.030	-2.93	0.005
$S + \mathcal{C}$	FM	3.71	0.030	2.26	0.005
$S + \mathcal{C}$	AFM	3.72	0.030	-1.44	0.005
$S + \mathcal{C}$ (LDA + $U$ )	FM	4.32	0.030	1.34	0.005

[Figs. 1(a) and 1(b)], it shows many features of the host band structure. Most important, however, a nondispersive band is found at about  $-0.4$  eV, i.e., at the experimental binding energy. The spin-up channel of the  $S + \mathcal{C}$  structure is similar to the spin-up channel of the  $S$  structure and is not shown.

Since the band structures depicted in Fig. 1 reflect the properties of the spectral density, it is instructive to consider the  $\mathbf{k}$  dependence of this quantity. In Fig. 2, we present the spectral density for two  $\mathbf{k}$  points. In the presented energy interval, both curves are characterized by two peaks. The position of one of the peaks depends strongly on the  $\mathbf{k}$  point. This peak corresponds to the strongly dispersive band originating from the semiconductor matrix. On the other hand, the position of the second peak does not depend on the wave vector, and the corresponding band is weakly dispersive.

The low spectral weight of the weakly dispersive peak reveals the impurity-related nature of the corresponding band. To verify the connection between the interstitial Mn

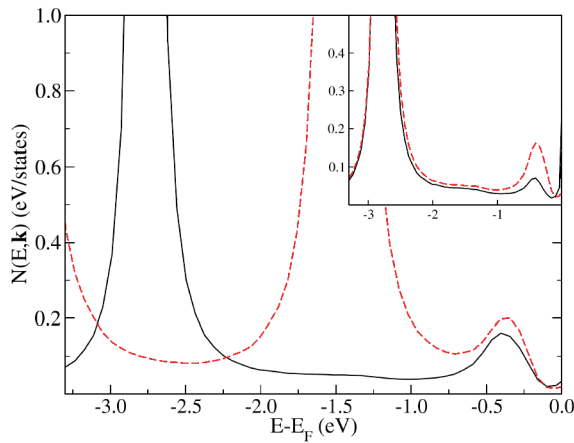


FIG. 2 (color). Spin-averaged spectral density of  $\text{Ga}_{0.965}\text{Mn}_{0.03}^S\text{Mn}_{0.015}^C\text{As}$  at the middle of a  $\Gamma$ - $X$  interval (dashed line) and at point  $X$  (solid line). Inset: Spectral density at point  $X$  for concentrations of the interstitial Mn  $x_C = 0.005$  (solid line) and  $x_C = 0.015$  (dashed line).

impurities and the weakly dispersive band, we compare in the inset in Fig. 2 the spectral density for two systems that differ by the concentration of the interstitial defects only. The large peak is not influenced by the threefold increase of the concentration of interstitial Mn, whereas the height of the peak corresponding to the weakly dispersive band is almost proportional to this concentration. This result explains the puzzle of the low experimental Mn-3d spectral weight of the weakly dispersive band by the low concentration of the interstitial impurities.

The weakly dispersive band is obtained also for the antiparallel relative orientation of the magnetic moments of the substitutal and interstitial Mn atoms. The band appears always in the spin-down channel with respect to the direction of the atomic moment of the interstitial Mn atoms. To further verify the robustness of the band position, we simulated the effect of atomic relaxation by changing interatomic distances around the interstitial Mn by the value up to  $\pm 10\%$ . Also, the paramagnetic phase was studied within the DLM scheme. The shift of the band was in all cases of the order of  $\pm 0.1$  eV. Hence, the band appears rather robust against these variations in the atomic and magnetic structure.

Our next purpose is to reveal the origin of the relation between the interstitial  $\mathcal{C}$ -Mn and the formation of the weakly dispersive band. The analysis of the atomic magnetic moments collected in Table I shows that interstitial Mn has a reduced magnetic moment compared to substitutal Mn. Further,  $m_C$  is always smaller than  $m_A$ . The difference in the magnetic moments is explained by the different atomic environment of the atoms. As a result, the crystal-field splitting of the Mn-3d states and the hybridization of these states with semiconductor states occur differently. Since the majority states of all types of Mn atoms are occupied, the reduction of the interstitial magnetic moments is a consequence of an increased occupation of the minority states of the interstitial Mn.

Summarizing, the weak dispersion of the band is explained by a mainly 3d character of the corresponding electron states. The position of the band at a small energy distance below the Fermi energy is explained by an increased occupation of the minority-spin states related to the decreasing value of the spin moment of Mn at interstitial sites  $\mathcal{C}$ . The low Mn-3d spectral weight of the weakly dispersive band is explained by the low concentration of the interstitial Mn atoms.

Thus, our LDA calculations suggest a consistent picture of the physical nature of the weakly dispersive energy band in the Fermi-level region. Since the intra-atomic electron correlations can be important for Mn-3d states, we performed additional calculations within the LDA +  $U$  method [17] where, in distinction to the standard LDA approach, the on-site Coulomb repulsion of electrons is explicitly accounted for through the parameter  $U$ . The  $U$  value was taken equal to 3 eV. Effectively, the on-site  $U$  tends to shift the occupied Mn-3d states by  $\frac{U}{2}$  to lower

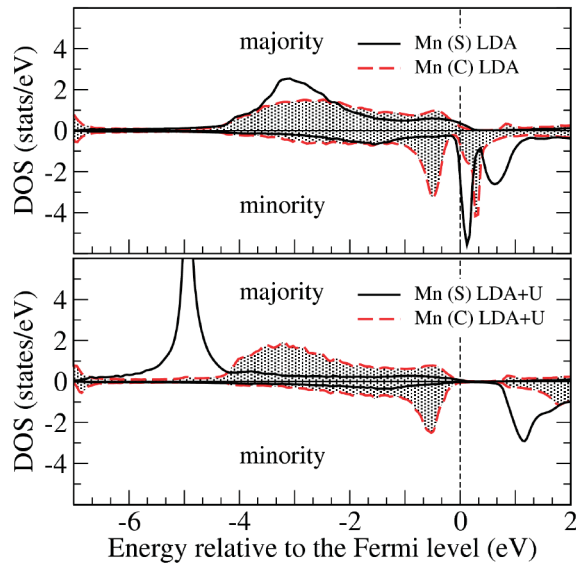


FIG. 3 (color). Partial Mn density of states of  $\text{Ga}_{0.965}\text{Mn}_{0.03}^{\text{S}}\text{Mn}_{0.005}^{\text{C}}\text{As}$  for substitutional (S) and interstitial (C) atoms. The upper panel presents the results of the LDA calculation, the lower panel the results of the LDA +  $U$  calculations.

energies while the empty Mn-3d states by  $\frac{U}{2}$  to higher energies. The calculational procedure is, however, iterative and takes into account the complex pattern of the hybridizations in the system.

In Fig. 3, we compare the partial density of states (DOS) of the substitutional and interstitial Mn for  $\text{Ga}_{0.965}\text{Mn}_{0.03}^{\text{S}}\text{Mn}_{0.005}^{\text{C}}\text{As}$  obtained within both LDA and LDA +  $U$  calculations. We see that there is substantial difference in the two DOS. For example, the main peak of the majority-spin 3d states of the substitutional Mn moved to lower energy and assumed the position about  $-4.9$  eV, that is, in rather good agreement with the experiment by Okabayashi *et al.* [10]. A striking feature is, however, a strong similarity of the occupied parts of the 3d DOS of the interstitial Mn in both calculational approaches. In particular, the position of the peak in the minority-spin channel corresponding to the weakly dispersive band is at a very similar energy. The weakly dispersive band calculated with the LDA +  $U$  method is in as good agreement with the experiment as in the LDA calculation (Fig. 1). Our conclusions about the nature of the weakly dispersive band remain valid: The energy position just below the Fermi level is determined by the reduced magnetic moment (Table I).

The stability of the properties of the weakly dispersive band with respect to the method applied in the calculations is highly nontrivial. The analysis of the iterative LDA +  $U$  process shows that in the first iteration  $U$  leads to the shift of the weakly dispersive band to lower energies by a large value close to  $\frac{U}{2}$ . The change of the electron structure

under the influence of  $U$  results in an increase of the number of the occupied 3d states of the interstitial Mn. This, in turn, causes the change of the electron Coulomb potential that leads to an increased position of the 3d states. Thus, the shift downwards because of  $U$  is compensated by the opposite shift because of the increased number of the 3d electrons.

In summary, we suggest a model which explains the nature of the weakly dispersive band near the Fermi level observed in the photoemission experiment. The band originates from the minority-spin 3d states of interstitial manganese surrounded by gallium atoms. Our model suggests the experimental observation of the band in a GaMnAs sample as a convenient indicator of the presence of the interstitial Mn impurities. On the other hand, our study shows that the control over defects in DMS allows one to formulate the task of the electron-structure “engineering” by design of the materials with highly spin-polarized electron bands in the Fermi-level region. Such materials have an enormous importance for the spintronics applications.

Interesting discussions with Patrick Bruno and Holger Meyerheim are acknowledged.

\*Electronic address: aernst@mpi-halle.de

- [1] G. A. Prinz, *Science* **282**, 1660 (1998).
- [2] M. Ohno, *Phys. Rev. B* **58**, 12 795 (1998).
- [3] K. W. Edmonds *et al.*, *Phys. Rev. Lett.* **92**, 037201 (2004).
- [4] T. Dietl, H. Ohno, F. Matsukura, J. Cibert, and D. Ferrand, *Science* **287**, 1019 (2000).
- [5] P. M. Krstajic, F. M. Peeters, V. A. Ivanov, V. Fleurov, and K. Kikoin, *Phys. Rev. B* **70**, 195215 (2004).
- [6] *Solid-State Photoemission and Related Methods. Theory and Experiment*, edited by W. Schattke and M. A. Van Hove (Wiley-VCH, Weinheim, 2003).
- [7] J. Okabayashi, A. Kimura, O. Rader, T. Mizokawa, A. Fujimori, T. Hayashi, and M. Tanaka, *Phys. Rev. B* **64**, 125304 (2001).
- [8] P. Weinberger, *Electron Scattering Theory of Ordered and Disordered Matter* (Clarendon, Oxford, 1990).
- [9] H. Åsklund, L. Ilver, J. Kanski, J. Sadowski, and R. Mathieu, *Phys. Rev. B* **66**, 115319 (2002).
- [10] J. Okabayashi, A. Kimura, T. Mizokawa, A. Fujimori, T. Hayashi, and M. Tanaka, *Phys. Rev. B* **59**, R2486 (1999).
- [11] O. Rader *et al.*, *Phys. Rev. B* **69**, 075202 (2004).
- [12] B. L. Gyorffy, A. J. Pindor, J. Staunton, G. M. Stocks, and H. Winter, *J. Phys. F* **15**, 1337 (1985).
- [13] K. M. Yu, W. Walukiewicz, T. Wojtowicz, I. Kuryliszyn, X. Liu, Y. Sasaki, and J. K. Furdyna, *Phys. Rev. B* **65**, 201303(R) (2002).
- [14] F. Maca and J. Masek, *Phys. Rev. B* **65**, 235209 (2002).
- [15] J. Masek and F. Maca, *Phys. Rev. B* **69**, 165212 (2004).
- [16] R. Wu, *Phys. Rev. Lett.* **94**, 207201 (2005).
- [17] V. I. Anisimov, J. Zaanen, and O. K. Andersen, *Phys. Rev. B* **44**, 943 (1991).